Crystallization of Poly(ethylene oxide) and Melt-Miscible PEO Blends

Limin Wu,[†] Melissa Lisowski,[‡] Sapna Talibuddin,[§] and James Runt*

Department of Materials Science & Engineering, The Pennsylvania State University, University Park, Pennsylvania 16802

Received July 24, 1998

ABSTRACT: Spherulitic growth rates for poly(ethylene oxide) and four model, melt-miscible blends were measured over a range of crystallization temperatures. The miscible diluents fall into two classes: those exhibiting relatively weak intermolecular interactions with PEO and those exhibiting strong interactions. Generally, at a given crystallization temperature, growth rates for blends with the strongly interacting polymers are considerably lower than those with weakly interacting polymers with comparable T_gs. To a first approximation, growth rates for PEO and the blends can be "superposed" when normalized by the degree of supercooling and $T - T_g$. In addition, at higher T_c and diluent concentrations, particularly for blends with strongly interacting diluents, the growth rate slows from $G \propto t^0$ to $G \propto t^{-1/2}$, consistent with a crossover to diffusion-controlled growth. Analysis of PEO growth rates using the LHM model yields $\sigma_e \sim 40$ ergs/cm^2 for crystallization in regime II. For the blends, the mobility as a function of T_c and diluent content was estimated from experimental growth rates and the nucleation constant for neat PEO. These mobilities were found to correlate well with diluent (or blend) T_g.

1. Introduction

In the past several years, we have used small-angle X-ray scattering to explore the development and final microstructure of melt-miscible blends of poly(ethylene oxide) (PEO).[1−3] Miscible amorphous polymers were chosen to exhibit relatively weak (poly(methyl methacrylate) (PMMA) and poly(vinyl acetate) (PVAc)) or strong (ethylene−methacrylic acid (EMAA) and styrene−hydoxystyrene (SHS) copolymers) intermolecular interactions with PEO. In each of these cases, one of the amorphous polymers was chosen to have a relatively low glass transition temperature, T_g (PVAc and EMAA), and the other a relatively high T_g (PMMA and SHS). Much of this earlier work was conducted on specimens crystallized at a temperature (T_c) of 45 °C. Not surprisingly, it was found that amorphous polymer mobility was the controlling factor determining diluent placement in the weakly interacting blends: PMMA was found to be completely incorporated between PEO lamellae while it was concluded that PVAc was at least partially excluded to interfibrillar regions. Strong intermolecular interactions were found to promote diluent exclusion as a result of a significant reduction in equilibrium melting point. This resulted in a very large decrease in spherulite growth rates, allowing more time for the strongly interacting diluent polymers to diffuse from the growth front. Even the high molecular weight, high T_g SHS copolymer diffused over relatively large length scales at blend concentrations of 20% SHS.[2] These observations are in general agreement with ideas first proposed by Keith and Padden.[4−6]

In the present paper we report on a continuation of our study of these "model" PEO blends. Here we focus on spherulite growth, particularly the influence of strong intermolecular interactions.

2. Experimental Section

Materials and Sample Preparation. The polymers used in this study were identical to those used in our previous work.[1−3] PEO of viscosity-average molecular weight 1.44×10^5 was obtained from Polysciences. The two weakly interacting polymers, PMMA and PVAc, were purchased from Aldrich and had measured T_gs of 113 and 31 °C, respectively. The two strongly interacting copolymers, EMAA and SHS, were supplied respectively by duPont[7] and Hoechst Celanese. The EMAA copolymer contained 55 wt % methacrylic acid units while SHS consisted of 50 wt % styrene and *p*-hydroxystyrene. The measured T_gs were 36 and 150 °C, respectively. Molecular weights and polydispersities for the amorphous polymers are reported in refs 1−3.

Films of PEO and PEO blends with the four miscible polymeric diluents were prepared by casting from two weight percent solutions in a suitable solvent: 50/50 THF/CH_2Cl_2 for PEO, PEO/EMAA, and PEO/PVAc, 50/50 THF/$CHCl_3$ for PEO/SHS, and $CHCl_3$ for PEO/PMMA. The blend solutions were stirred for 2 days at room temperature and then were cast onto clean glass slides. The resulting films were dried in air at room temperature for 24 h and then under vacuum at 80 °C for 24 h to ensure complete solvent removal.

Spherulitic Growth Rate Measurements. The dried films were heated to 100 °C for 3 min in a Mettler hot stage (model FP-82) to erase previous thermal history and then rapidly transferred to a second hot stage set at the desired crystallization temperature (T_c). In some cases the temperature of the second hot stage rose somewhat after placing the sample into it and then returned to the set temperature. In such cases, $t = 0$ was defined on return to the set temperature (T_c). The development of the spherulitic superstructure was viewed with an Olympus BHSP-300 microscope and the crystallization event recorded with a video camera and VCR. Crystallization was monitored for time periods from a few minutes to as long as 30 h (for PEO/SHS blends crystallized at relatively high T_c). In the cases where spherulite radii (R) increased linearly with time, the average spherulite growth rate (G) was determined from the slope of the R vs t relationship for from 1 to 5 spherulites. In the case of nonlinear growth, G was determined at the onset of spherulite growth.

3. Results and Discussion

PEO. Spherulite growth rates for PEO over a range of crystallization temperatures are shown in Figure

[†] Present address: Department of Materials Science, Fudan University, Shanghai, PRC.
[‡] Present address: Montel Polyolefins, Elkton, MD 21921.
[§] Present address: GE Plastics, Mt. Vernon, IN 47620.
* To whom correspondence should be addressed.

10.1021/ma981169o CCC: $18.00
Published on Web 02/19/1999

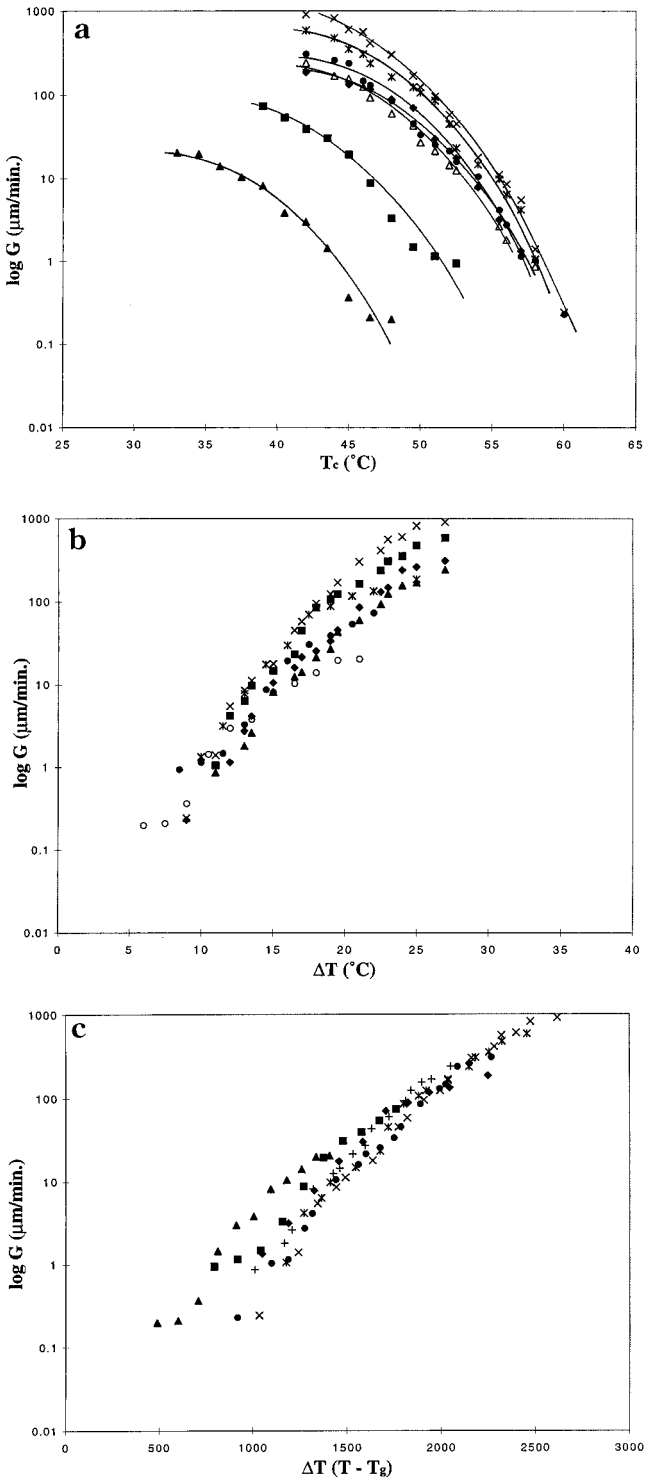

Figure 1. (a) Log spherulite growth rates vs T_c for PEO and blends with low T_g amorphous polymers: ×, PEO; ∗, 90 PEO/10PVAc; ●, 80/20 PVAc; △, 70/30 PVAc; ◆, 90/10 EMAA; ■, 80/20 EMAA; ▲, 70/30 EMAA. (b) Log spherulite growth rates vs degree of supercooling for PEO and blends with low T_g amorphous polymers: ×, PEO; ■, 90 PEO/10PVAc; ◆, 80/20 PVAc; ▲, 70/30 PVAc; ∗, 90/10 EMAA; ●, 80/20 EMAA; ○, 70/30 EMAA. (c) Log spherulite growth rates vs $\Delta T(T - T_g)$ for PEO and blends with low T_g amorphous polymers: ×, PEO; ∗, 90 PEO/10PVAc; ●, 80/20 PVAc; +, 70/30 PVAc; ◆, 90/10 EMAA; ■, 80/20 EMAA; ▲, 70/30 EMAA.

1a: G changes by about 4 orders of magnitude over the ~20 °C interval of T_c explored in our studies. Growth rates were analyzed using the Lauritzen−Hoffman−Miller (LHM) kinetic theory:[8,9]

$$G = G_0(\Delta T) \exp(-U^*/R(T_c - T_\infty)) \exp(-K_g/T_c f(\Delta T)) \quad (1)$$

where ΔT is the degree of supercooling ($T_m^0 - T_c$), U^* the activation energy for transport of segments across the melt−crystal interface, R the gas constant, T_∞ the temperature below which all viscous flow ceases (taken here as $T_g - 30$ K), and f a function that accounts for the temperature dependence of the heat of fusion [$f = 2T_c/(T_m^0 + T_c)$]. K_g is the nucleation constant and is defined as $K_g = n_i b_0 \sigma \sigma_e T_m^0/k\Delta H_f^0$, where n_i is 4 for crystallization regimes I and III and 2 for regime II, b_0 is the layer thickness, σ and σ_e are the lateral and end surface free energies, respectively, ΔH_f^0 is the perfect crystal heat of fusion, and k is the Boltzmann constant.

In our analysis, ΔH_f^0 was taken as 203 J/g,[10] b_0 = 0.465 nm,[11] and $T_g = -55$ °C.[2] Although there is some controversy in the literature as to the precise value of T_m^0 for high molecular weight PEO, 69 °C appears to be the most generally accepted.[12,13] A plot of $\ln G + U^*/R(T_c - T_\infty) - \ln \Delta T$ vs $1/T_c f(\Delta T)$ (the so-called LH plot) yields the nucleation constant, K_g (the slope), and $\ln G_0$ (the intercept). Figure 2 presents the LH plot for the PEO data in Figure 1, using $U^* = 1.5$ kcal/mol.[9,14] Although regime transitions have been reported for PEO crystallized in a similar T_c range in several publications,[13,15,16] no such transition(s) is observed in Figure 2, although there appears to be some curvature in the plot. If two lines are fit through the data at high and low T_c, a "break" occurs at about 54 °C. This is near where a regime II−III transition has been reported for narrow PEO fractions.[13] However, treating this as a regime II−III transition, the ratio of the nucleation constants would be ~1.4, well below the predicted value of 2 for a regime II−III transition.[8,9] The ratio increases if a larger value for U^* is assumed, but there is little justification for doing so (see, e.g., ref 14). It has been proposed that the break in the growth rate T_c relationship near 50 °C is associated with a change in morphology (crystallographic orientation of the growth front) and not a regime transition.[17,18]

The best fit of a linear relationship to the data in Figure 2 yields $K_g = 3.80 \times 10^4$ K^2 and $\ln G_0 = 14.0$. Determination of the surface free energy product, $\sigma\sigma_e$, in situations such as that in Figure 2 is complicated by the uncertainty of the crystallization regime. In principle, one can use the so-called Lauritzen Z-test[19] to discriminate between regimes I and II, but regime III is not considered in this approach. A Z-test is performed in practice by using the K_g values derived from LH plots and inequalities for Z, to estimate the range of substrate length values (L') for regime I or regime II. The regime is then determined by deciding whether the range of L' values calculated in each case is reasonable. However, another difficulty is in determining what constitutes a reasonable value for L' in each regime. Polyethylene is the only polymer for which L' has been estimated, and what is considered reasonable at the regime I to II transition has varied somewhat over time. A value within a factor of 1.5 of ~87 nm is the most recent estimate.[8] Values of L' calculated from the experimental K_g for PEO bracket the "expected" value, while calculations assuming regime I lead to L' values that are much too small.

Assuming that crystallization in the T_c range covered by Figure 2 follows regime II kinetics, we find $\sigma\sigma_e$ = 401 ergs^2/cm.[4] This is within about 10% of the value reported by Kovacs et al.[14] (450 ergs^2/cm,[4] also assuming

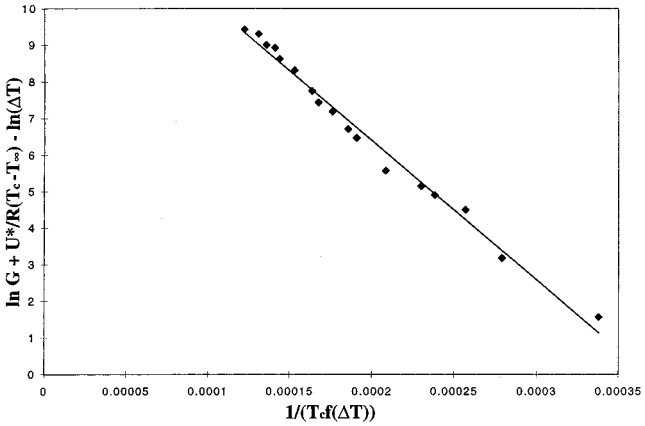

Figure 2. LH plot for neat PEO (using $U^* = 1.5$ kcal/mol and $T_m^0 = 69$ °C).

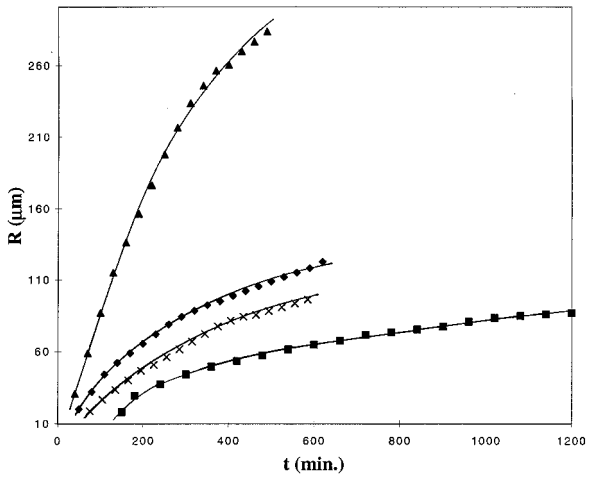

Figure 3. Spherulite radii vs time for four strongly interacting PEO blends: ▲, 80/20 PEO/EMAA, $T_c = 52.5$ °C; ◆, 80/20 SHS, $T_c = 55.5$ °C; ×, 70/30 EMAA, $T_c = 48$ °C; ■, 70/30 SHS, $T_c = 46.5$ °C.

regime II). Taking $\sigma \sim 10$ ergs/cm^2 [13] (close to the value one would obtain by using the Thomas−Stavely relationship[20] with $\alpha = 0.1$) leads to $\sigma_e \sim 40$ ergs/cm^2. This is very similar to that reported by Hoffman[21] from an analysis of the experimental data of Kovacs et al.[14,22] for low molecular weight, melt-crystallized PEO (42 ergs/cm^2). The work of chain folding (q) is related to σ_e by $q = 2\sigma_e A_0$, where A_0 is the cross-sectional area of the chain.[8] For $A_0 = 0.214$ nm,[213] $q \sim 2.5$ kcal/mol folds, a value which is similar to that determined previously for other polyethers with flexible chain backbones.[9,23] Alternatively, if it is assumed that the data in Figure 2 conform to regime III kinetics, $\sigma_e \sim 20$ ergs/cm^2. This seems to be unrealistically small however since this leads to a work of chain folding on the order of 1 kcal/mol.

Miscible PEO Blends. For the majority of blends and T_cs under consideration here, typical linear R vs t behavior is observed (i.e., $G \propto t^0$). This implies constant diluent concentration at the growth fronts throughout the course of crystallization. However, for a few PEO blends with PVAc, and particularly for the slowly crystallizing blends with EMAA and SHS, nonlinear R vs t behavior is observed at the highest T_cs and diluent concentrations. Selected examples for the strongly interacting blends are shown in Figure 3. This type of behavior has been observed previously in mixtures exhibiting a combination of relatively slow spherulite growth and relatively mobile diluents.[5,24] The implication is that there is an increasing concentration of diluent in the mother phase as crystallization proceeds (due to radial diffusion of the diluent) and hence slower spherulite growth as crystallization continues. For blends with strongly interacting (or low molecular weight) diluents, the degree of supercooling will also be continually depressed.

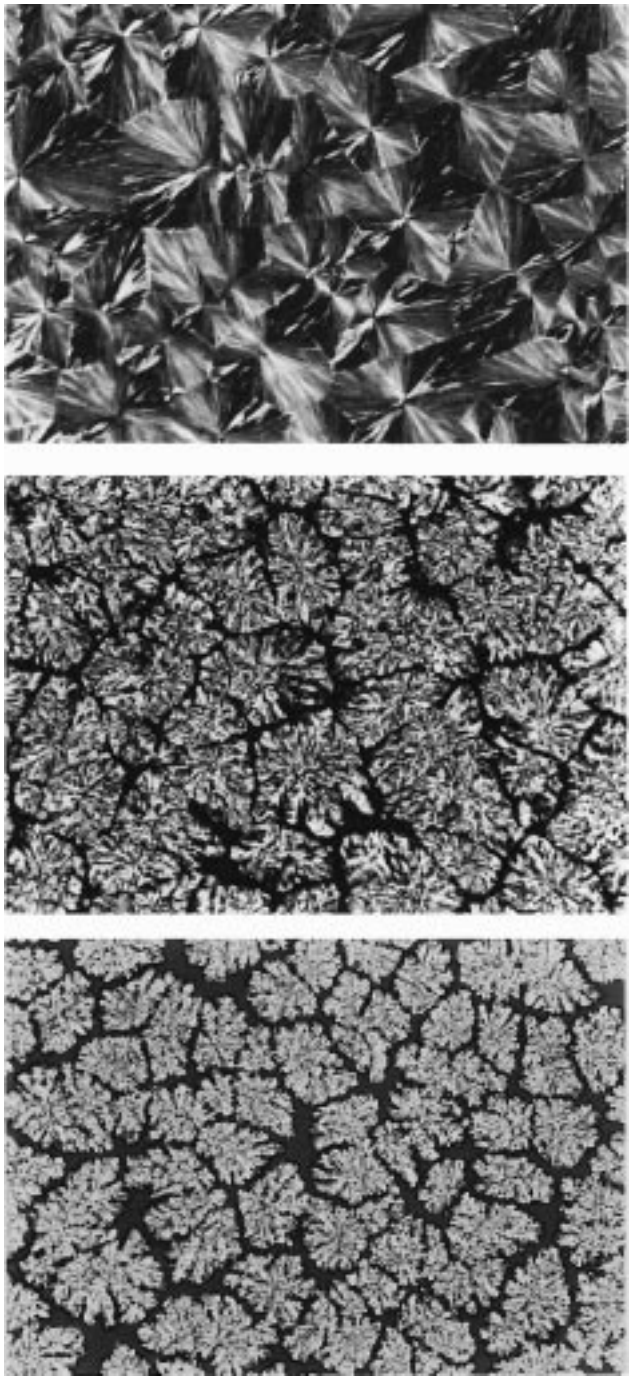

Figure 4. Optical micrographs (100×) of (a, top) 90/10 PEO/SHS blend crystallized at 52.5 °C, (b, middle) 80/20 PEO/SHS blend crystallized at 55.5 °C (for 18 h), and (c, bottom) 70/30 PEO/SHS blend crystallized at 46.5 °C (for 24 h).

As will be discussed below, G is severely depressed for blends with the strongly interacting diluents, permitting even high T_g, high molecular weight SHS to diffuse over relatively long distances during the course of crystallization. This is illustrated in the optical micrographs in Figure 4. [For reference to the morphol-

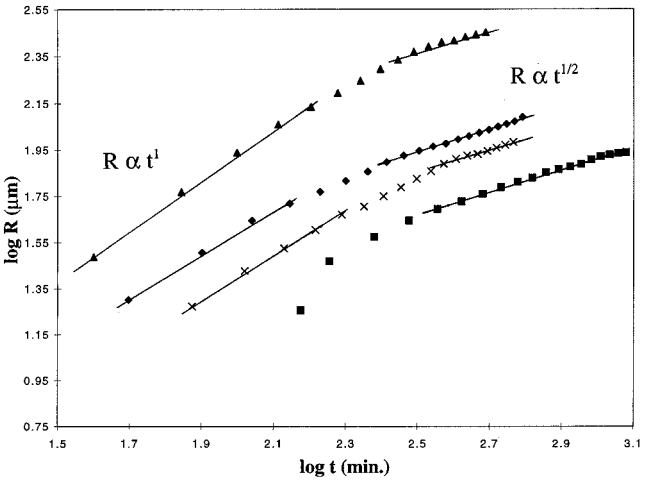

Figure 5. log R vs log t for data in Figure 3: ▲, 80/20 PEO/EMAA; ◆, 80/20 SHS; ×, 70/30 EMAA; ■, 70/30 SHS.

ogy of neat PEO at a variety of molecular weights and T_cs, see ref 25.] The first micrograph shows the typical compact spherulitic morphology at the conclusion of crystallization of a 90/10 PEO/SHS blend crystallized at 52.5 °C. This structure developed in about 20 min. Figure 4b shows the morphology of an 80/20 SHS blend crystallized at 55.5 °C after 18 h at T_c. The growth units are clearly coarser and non-volume filling. As seen in Figure 3, growth slows during the course of morphology development, which is consistent with significant buildup of SHS in interspherulitic regions. Even after quenching to room temperature, no additional crystallization is observed in the interspherulitic regions, consistent with a relatively high concentration of SHS. A similar final morphology is observed for a 70/30 SHS mixture, crystallized at 46.5 °C. These observations are in general agreement with the observations and ideas proposed by Keith and Padden.[4−6]

Figure 5 shows the data reported in Figure 3 but plotted as log R vs log t. At short times, linear regression yields $R \propto t^1$; i.e., G is constant with time. At the longest times where growth slows, there is a crossover to $R \propto t^{1/2}$ ($G \propto t^{-1/2}$) for all four blends in Figure 5. This indicates a change to diffusion-controlled growth at longer times.[26] Similar behavior has been reported previously by Okada et al.[23] and Lee[27] for polymer/oligomer mixtures.

Figure 1a summarizes the measured spherulite growth rates for PEO and the blends with the two "low T_g" amorphous polymers, PVAc and EMAA. Measurements were made for blends containing 10, 20, and 30% diluent polymer. There is a precipitous drop in growth rate for EMAA blends compared to that of PEO: at comparable T_c, G decreases by more than 3 orders of magnitude for the 30% EMAA blend. An important part of this decrease is related to the significant equilibrium melting point depression ($\Delta T_m^0 = T_m^0 - T_m^{0\prime}$, where $T_m^{0\prime}$ is the equilibrium melting point of PEO in the blend environment) for PEO blends containing amorphous polymers capable of forming strong intermolecular interactions. However, it is difficult in practice to determine reliable $T_m^{0\prime}$.[28] PVAc is considered to be relatively weakly interacting, and changes in $T_m^{0\prime}$ with blend composition are assumed to be negligible for the present purposes. $T_m^{0\prime}$ for EMAA blends was estimated as follows.[2] From the LHM theory of crystallization[8,20]

$$l_c = \beta l_g^* = \beta[2\sigma_e T_m^\circ/\Delta H_f^\circ \Delta T] \quad (2)$$

where l_g^* is the initial crystal thickness and β the factor by which the crystals thicken at T_c. If it is assumed that β and σ_e are independent of blending, and recognized that changes in T_m° (in kelvin units) have only a relatively small effect on l_c in eq 2, then $l_c = z(1/\Delta T)$, where z is a constant for PEO and the blends. This then permits an estimation of the degree of supercooling at which the EMAA (and SHS) blends were crystallized by comparing the experimental crystal thicknesses with those determined by Arlie et al. for neat PEO.[29] Further details of this analysis are described in ref 2.

Since the 70/30 EMAA blend was not considered in ref 2 and the measured crystal thickness for the 90/10 blend is difficult to distinguish from that of PEO due to experimental uncertainty, we took the following approach in estimating $T_m^{0\prime}$ for the EMAA blends. Using the procedure summarized above, the measured l_c for the 80/20 EMAA blend (at $T_c = 45$ °C) was compared to the data of Arlie et al.,[29] and a T_m^o of ∼61 °C was estimated ($\Delta T_m^0 = 8$ °C). With this information, we then used the expression of Nishi and Wang[30] to estimated $T_m^{0\prime}$ for the 90/10 and 70/30 blends (≈67 and 54 °C, respectively).

Figure 1b presents the growth rate data for the "low T_g" blends vs ΔT ($= T_m^{0\prime} - T_c$) using the $T_m^{0\prime}$ estimated above. The spread in the data collapses down to within about an order of magnitude of PEO, demonstrating the relative importance of ΔT_m^0 for these blends. If the data are further normalized by $T - T_g$ in a first-order attempt to account for transport in the melt, we arrive at the behavior displayed in Figure 1c. Considering the uncertainty in the estimated T_m^0s and T_gs (estimated using the Fox−Flory relationship[31]) and the lack of details regarding mutual diffusion of the component polymers, Figure 1c represents reasonable "master curve" behavior.

Figure 6a summarizes the growth rate vs T_c relationship for the blends containing the "high T_g" diluent polymers. Again, the strongly interacting diluent, SHS, results in a very significant reduction in G compared to the case of PEO at comparable T_c (a decrease of about 4 orders of magnitude near $T_c = 45$ °C). Changes in crystal thickness for the SHS blends are not as large as for PEO/EMAA, suggesting that the melting point depression is not as large, but still very significant.[2] Using the same approach as above to determine T_m^0, we arrive at 67, 63, and 56 °C respectively for blends containing 10, 20, and 30% SHS. The corresponding growth rates normalized by ΔT (Figure 6b) are not well superposed, as expected since the transport term is significant in these cases. Normalizing on the basis of $\Delta T(T - T_g)$ provides a first-order superposition of the experimental growth rate data (Figure 6c).

Spherulite growth rates in miscible blends are frequently analyzed by a modified LHM expression:[32]

$$G = \phi_2 G_0(\Delta T) \exp(-U^*/R(T_c - T_\infty)) \times \exp(-K_g/T_c f(\Delta T) + 0.2 T_m^{0\prime} \ln \phi_2/\Delta T) \quad (3)$$

where ϕ_2 is the volume fraction of the crystalline polymer. The last term on the right-hand side of eq 3 is a simplified form of an expression representing the entropic contribution to the free energy required to form a nucleus of critical size.[32] The prefactor ϕ_2 is appropriate for regimes I and III, since the surface nucleation

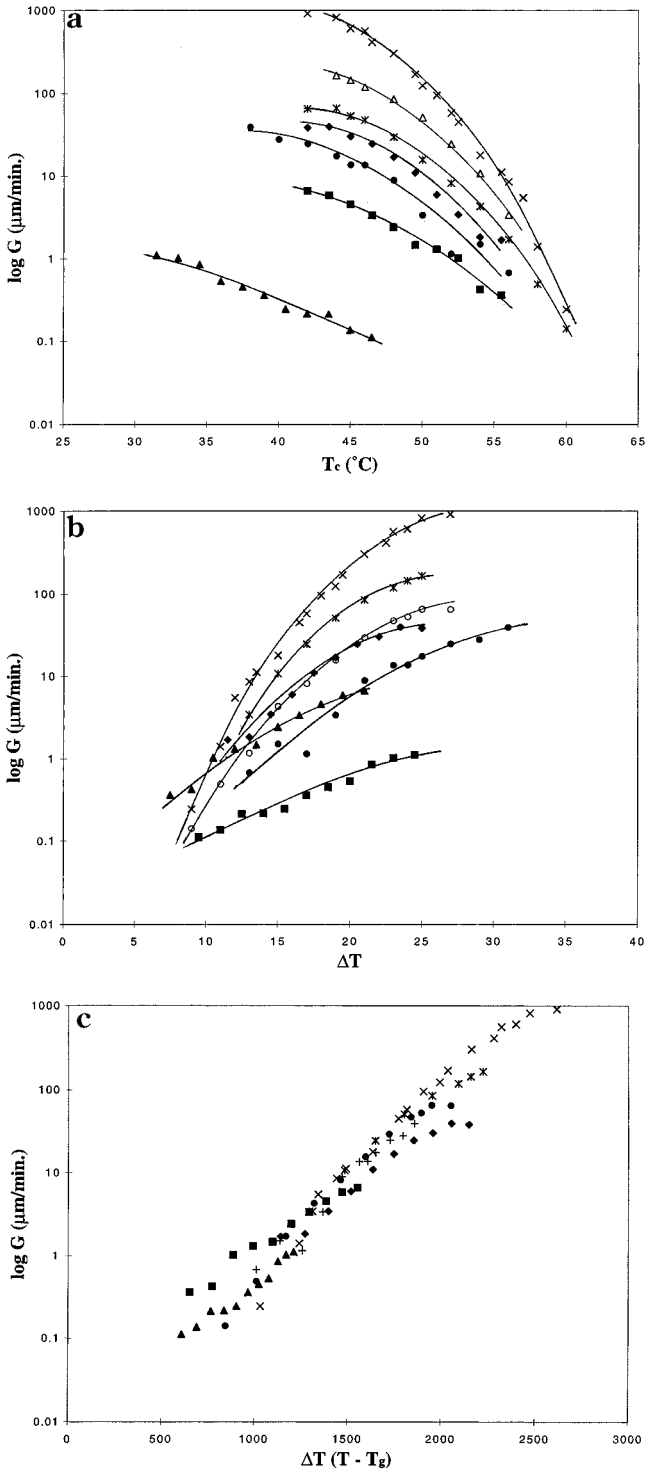

Figure 6. (a) Log spherulite growth rates vs T_c for PEO and blends with high T_g amorphous polymers: ×, PEO; Δ, 90 PEO/10 PMMA; ∗, 80/20 PMMA; ●, 70/30 PMMA; ◆, 90/10 SHS; ■, 80/20 SHS; ▲, 70/30 SHS. (b) Log spherulite growth rates vs degree of supercooling for PEO and blends with high T_g amorphous polymers: ×, PEO; ∗, 90 PEO/10 PMMA; ○, 80/20 PMMA; ●, 70/30 PMMA; ◆, 90/10 SHS; ▲, 80/20 SHS; ■, 70/30 SHS. (c) Log spherulite growth rates vs $\Delta T(T - T_g)$ for PEO and blends with high T_g amorphous polymers: ×, PEO; ∗− 90 PEO/10 PMMA; ●, 80/20 PMMA; +, 70/30 PMMA; ◆, 90/10 SHS; ■, 80/20 SHS; ▲, 70/30 SHS.

rate (i) is proportional to the number of crystallizing molecules at the growth front and $G \propto i$ in regimes I and III. $G \propto i^{1/2}$ in regime II, and the appropriate prefactor in eq 3 is then $\phi_2^{1/2}$.[33] Using eq 3 to fit miscible blend growth data using the usual transport term

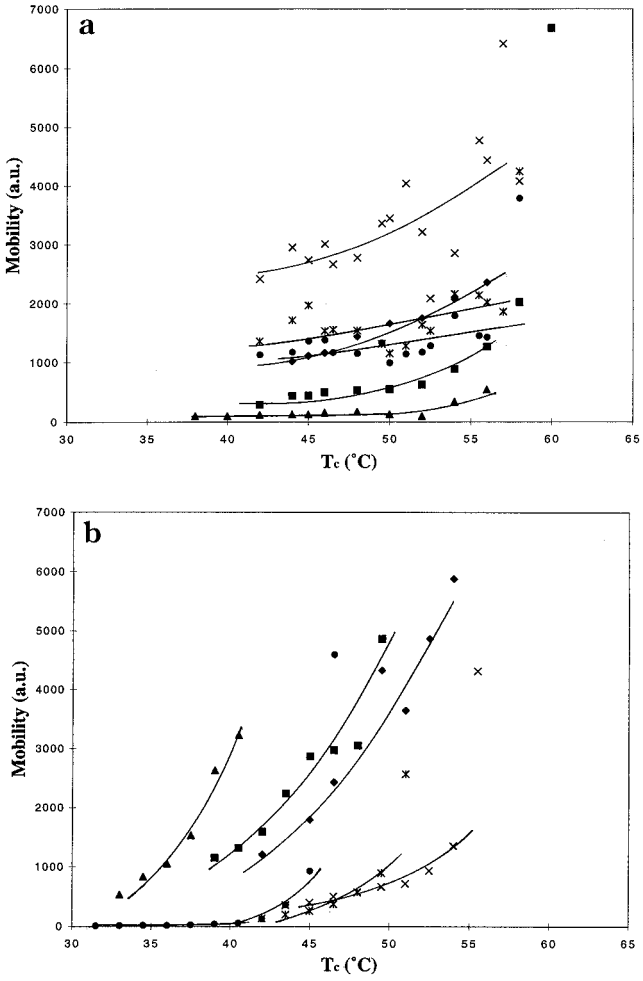

Figure 7. (a) Mobilities (β_g, in arbitrary units) vs T_c for weakly interacting blends: ×, 90 PEO/10 PVAc; ∗, 80/20 PVAc; ●, 70/30 PVAc; ◆, 90/10 PMMA; ■, 80/20 PMMA; ▲, 70/30 PMMA. (b) Mobilities (β_g, in arbitrary units) vs T_c for strongly interacting blends: ◆, 90 PEO/10 EMAA; ■, 80/20 EMAA; ▲, 70/30 EMAA; ×, 90/10 SHS; ∗, 80/20 SHS; ●, 70/30 SHS.

sometimes leads to an apparent change in K_g (and hence σ_e) for the miscible blend. Since σ_e is believed to be dominated by q[8,20] and the other parameters in the expression for K_g are not expected to change significantly on blending, a significant change in K_g on blending would not be anticipated (in the absence of a regime change).

An alternative approach has been proposed by Inoue et al.[33,34] For crystallization in regime II

$$G/(\phi_2^{1/2}\Delta T \exp(-K_g/T_c f(\Delta T))) \propto \beta_g \qquad (4)$$

where β_g is a mobility term describing the transport of crystallizable molecules to the growth front and is related to the mutual diffusion coefficient in the blend environment.[33,34] Taking K_g for the blend as that determined experimentally for the neat crystalline polymer, the chain mobility can be estimated from eq 4 from measured growth rates. This approach was used for the blends under consideration here. Parts a and b of Figure 7 present the calculated mobilities (β_g) for the weakly and strongly interacting blends, respectively. The behavior is qualitatively sensible in that β_g in blends with the lower T_g diluents are greater that those with higher T_g diluent polymers. Figure 8 presents a closer look at the calculated mobilities for PEO and 80/

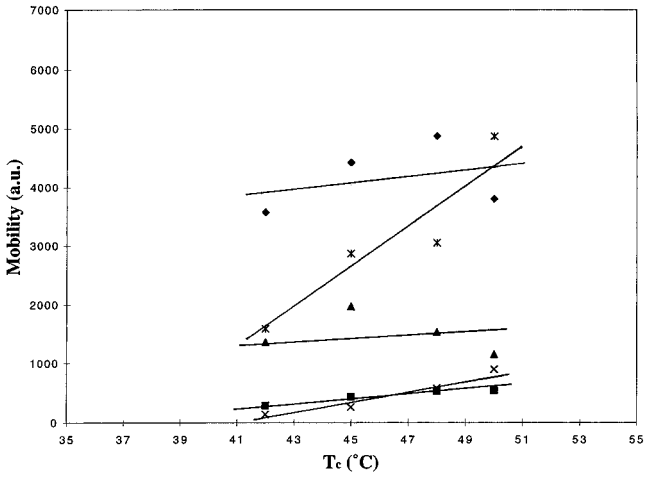

Figure 8. Mobilities (arbitrary units) vs T_c for PEO and 80/20 blends. Lines are for guidance purposes only. ◆, PEO; ∗, 80/20 EMAA; ▲, 80/20 PVAc; ■, 80/20 PMMA; ×, 80/20 SHS.

20 blends crystallized at temperatures between 40 and 50 °C. The behavior follows expectations based on differences in diluent T_g. The calculated mobilities of EMAA blends are somewhat higher than PVAc blends, consistent with the relatively lower EMAA molecular weight.

Acknowledgment. The authors acknowledge the donors of the Petroleum Research Fund, administered by the American Chemical Society, for their support of this work. We would also like to thank Prof. Ralph Colby for helpful discussions.

References and Notes

(1) Talibuddin, S.; Runt, J.; Liu, L.-Z.; Chu, B. *Macromolecules* **1998**, *31*, 1627.
(2) Talibuddin, S.; Wu, L.; Runt, J.; Lin J. S. *Macromolecules* **1996**, *29*, 7527.
(3) Barron, C. A. Ph.D. Thesis, The Pennsylvania State University, 1994.
(4) Keith, H. D.; Padden, F. J. *J. Appl. Phys.* **1964**, *35*, 1270.
(5) Keith, H. D.; Padden, F. J. *J. Appl. Phys.* **1964**, *35*, 1286.
(6) Keith, H. D.; Padden, F. J. *J. Polym. Sci., Polym. Phys. Ed.* **1987**, *25*, 2297.
(7) Lee, J. Y.; Painter, P. C.; Coleman, M. M. *Macromolecules* **1988**, *21*, 346.
(8) Hoffman, J. D.; Miller, R. L. *Polymer* **1997**, *38*, 3151.
(9) Hoffman, J. D.; Miller, R. L. *Macromolecules* **1988**, *21*, 3038.
(10) Wunderlich, B. *Macromolecular Physics*; Academic Press: New York, 1980; Vol. 3.
(11) Alfonso, G. C.; Russell, T. P. *Macromolecules* **1986**, *19*, 1143.
(12) Buckley, C. P.; Kovacs, A. J. *Prog. Colloid Polym. Sci.* **1975**, *58*, 44.
(13) Cheng, S. Z. D.; Chen, J.; Janimak, J. J. *Polymer* **1990**, *31*, 1018.
(14) Kovacs, A. J.; Straupe, C.; Gonthier, A. *J. Polym. Sci., Polym. Symp.* **1977**, *59*, 31.
(15) Richardson, P. H.; Richards, R. W.; Blundell, W. A.; MacDonald, W. A.; Mills, P. *Polymer* **1995**, *36*, 3059.
(16) Allen, R. C.; Mandelkern, L. *Polym. Bull.* **1987**, *17*, 473.
(17) Point, J.-J.; Damman, P.; Janimak, J. J. *Polymer* **1993**, *34*, 3771.
(18) Marentetee, J. M.; Brown, G. R. *Polymer* **1998**, *39*, 1405.
(19) Lauritzen, J. I., Jr. *J. Appl. Phys.* **1973**, *44*, 4353.
(20) Hoffman, J. D.; Davis, G. T.; Lauritzen, J. I. In *Treatise in Solid State Chemistry*; Hannay, H. B., Ed.; Plenum Press: New York, 1975; Vol. 3.
(21) Hoffman, J. D. *Macromolecules* **1986**, *19*, 1124.
(22) Kovacs, A. J.; Gonthier, A.; Straupe, C. *J. Polym. Sci., Polym. Symp.* **1975**, *57*, 283.
(23) Runt, J.; Wagner, R. F.; Zimmer, M. *Macromolecules* **1987**, *20*, 2531.
(24) Okada, T.; Saito, H.; Inoue, T. *Macromolecules* **1990**, *23*, 3865.
(25) Allen, R. C.; Mandelkern, L. *J. Polym. Sci., Polym. Phys. Ed.* **1982**, *20*, 1465.
(26) Frank, F. C. *Proc. R. Soc. London* **1950**, *A201*, 586.
(27) Lee, C. H. *Polymer* **1998**, *39*, 5197.
(28) Runt, J. In *Polymer Blends: Formulation and Performance*; Paul, D. R., Bucknall, C., Eds.; Wiley: New York, Chapter 6, in press.
(29) Arlie, J. P.; Spegt, P.; Skoulios, A. *Makromol. Chem.* **1967**, *104*, 212.
(30) Nishi, T.; Wang, T. T. *Macromolecules* **1975**, *8*, 909.
(31) Fox, T. G. *Bull. Am. Phys. Soc.* **1956**, *1*, 123.
(32) Boon, J.; Azcue, J. M. *J. Polym. Sci., Polym. Phys. Ed.* **1968**, *6*, 885.
(33) Okamoto, M.; Inoue, T. *Polymer* **1995**, *36*, 2739.
(34) Okada, T.; Saito, H.; Inoue, T. *Polymer* **1994**, *35*, 5699.

MA981169O